Vietnam Journal of Mechanics, NCST of Vietnam Vol. 24, 2002, No 4 (219 – 235)

NUMERICAL SIMULATION OF POLLUTANT DISPERSION NEAR OBSTACLE BASED ON $k-\varepsilon$ TURBULENCE CLOSURE SCHEME

DUONG NGOC HAI AND NGUYEN THE DUC
Institute of Mechanics, NCST, 264 Doican, Hanoi, Vietnam

ABSTRACT. To simulate the wind field, pollutant transport and dispersion near an obstacle, a numerical code based on the $k-\varepsilon$ turbulence model has been built. Beside the standard $k-\varepsilon$, two other modifications proposed by Detering & Etling and Duynkerke are also considered. The calculation results are verified based on the measurement data of von Karman Institute for Fluid Dynamics (Belgium). Modifications of the turbulent Schmidt number were carried out in order to match the measured results. The code was used to investigate the influence of the recirculation zone behind a building of cubical shape on the transport and dispersion of pollutant. For a stack behind and near the obstacle, some conclusions about the effect of the stack height and stack location were derived.

1. Introduction

The need of atmospheric diffusion models, that are capable of accounting the effects of complex terrain, is great, because many industrial enterprises and major cities reside in such areas.

Topography modifies the near-field dispersion of atmospheric pollution through changes of the mean flow (affecting plume path), turbulence (affecting plume shape and rate of spread) and transport into, or release within recirculation zones. Many detailed field experiments and laboratory simulations have been conducted to examine these effects.

In Russia, development of simple diffusion models for complex terrain was begun in late 1960s. The approach pursued was based on the joint numerical integration of the equation of atmospheric diffusion and the system of equation of hydro-thermodynamics for the atmospheric boundary layer over curvilinear, thermally inhomogeneous underlying surfaces. This approach was employed by Berliand and Genikhovich [1].

Initial studies of terrain effects in United States were based on the modified Gaussian diffusion model. The simple dispersion models for the complex terrain make some assumptions about the effective plume centerline relative to the terrain. Examples include MPTER, COMPLEX, CTDM and TAPAS models ([2]-[5]). However, the disadvantages of these models are that realistic conditions (three-dimensional variations in the wind field and diffusivity) can not be simulated correctly by this way. Consequently, it is now recognized that in order to simulate

realistic wind field and diffusivity, it is necessary to solve the full set of fluid dynamic equations of mean properties (include pollutant concentration) using numerical methods.

Recent increases in computer power mean that numerical prediction of pollutant dispersion by solving the full system of transport and dispersion equations of the pollutants is now viable. Consideration of the equations of mean properties reduces the problem of turbulence closure ([6]-[8]).

The application of first-order closure (K theory) has been widespread (see e.g. [9]-[14]). The first-order closure model employs a diagnostic formula for the length scale or mixing length. As it is difficult to prescribe the mixing-length distribution in situations other than simple shear-layer flow, the first-order model is not suitable for flows with complex structure.

Second and higher order closure models employ transport equations for the Reynolds stresses and turbulent fluxes derived from the Navier-Stokes equations (see [6], [7], [15] and [16]). However, the resulting model is quite complex, which makes it less suitable for solving practical problems.

An intermediate one-and-half order closure model, so-called the $k-\varepsilon$ turbulence model (k referring to the turbulent kinetic energy, and ε referring to the dissipation rate), requires only two additional prognostic equations in comparison with the first-order closure model. It has been found that this model may be a successful compromise between capability and simplicity.

The standard model [17] has been shown to work quite well in the engineering field for many different flows not controlled by buoyancy forces. However, the atmospheric flows are affected by buoyancy forces strongly in many cases, so application of $k-\varepsilon$ model to atmospheric flows generally requires its modification. Even with these changes, however, the model constants are not constants but variables strongly depended on flow structure and buoyancy. Detering and Etling [18] compared their model calculations for the neutral atmospheric boundary layer with an experiment of the "Leipzig Wind Profile" and concluded that the eddy viscosity predicted by the standard $k-\varepsilon$ model were much too large. In order to match observed data, they modified the ε-equation by making one of the constants as function of the turbulent length scale, friction velocity and Coriolis parameter. Duynkerke [19] also modified the standard $k-\varepsilon$ model constant values on the basic of atmospheric data and considered the diffusion term as an additional production term in the ε-equation only when its value was positive.

In this study, a numerical code based on the $k-\varepsilon$ turbulence model has been built. The description of numerical model and the numerical methods of this code are presented in Sections 2 and 3. The code has been verified based on its application to simulate the wind field, pollutant transport and dispersion near a three-dimensional hill of conic shape. The calculation results are compared with the measurement data of von Karman Institute for Fluid Dynamics (VKI) of Belgium. Beside the standard $k-\varepsilon$, two other modifications proposed by Detering & Etling and Duynkerke are also

considered. The verification results and some concerned discussions are presented in Section 4.

For flow approaching to an obstacle, some recirculation zones may be created by flow separation from the edges of the obstacle. The largest recirculation zone is usually behind the obstacle. The existence of this zone strongly influences on the pollutant transport and diffusion around the obstacle. The pollutant's concentration at the ground surface may be very high as the sources are set in recirculation zones. The high air pollution near Ninh Binh thermal power station in the past, for example, is concerned with the recirculation zone behind Canh Dieu mountain. In the cities, these bad influences also may be observed near building or in street canyons. Because of undesirable recirculation zone's effects and the fail of simple dispersion model and hydrostatic models in this field, in this study, the numerical investigation was performed to investigate the influences on considered processes of stack height and location when the stack is set behind the obstacle - a cubical building. Results of these investigations and several concerned discussions are presented in Section 5. Finally, Section 6 summarizes the main conclusions of the work.

2. Description of models

Numerical model of flow based on the standard $k-\varepsilon$ turbulence closure scheme was presented in [20]. Two modifications of standard $k-\varepsilon$ turbulence closure scheme for the atmospheric application: Detering and Etling's modification and Duynkerke's modification were also presented in [21]. We do not describe them here again to economy space.

The transport equation for a passive pollutant in the turbulent flows can be written as follows:

$$\frac{\partial C}{\partial t}+U_i\frac{\partial C}{\partial x_i}=-\frac{\partial(\overline{u_i'c'})}{\partial x_i}+S, \tag{2.1}$$

where U_i are the components of mean velocity; u_i' are the components of turbulent velocity; C is the mean concentration; c' is the turbulent deviation of concentration and S is the mass generation rate. As usual for fully turbulent flows, the molecular diffusive transport terms are neglected in comparison with the similar term of turbulence.

In equation (2.1), the new expression $\overline{u_i'c'}$ describes the flux of substance due to turbulent motion. Mathematically, it represents a new unknown quantity. Therefore the problem is not closed and cannot be solved in a unique way.

The first order and $k-\varepsilon$ turbulence closure schemes assumed that the turbulent flux of substance is proportional to gradient of the mean concentration:

$$\overline{u_i'c'}=-K_i\frac{\partial C}{\partial x_i}, \tag{2.2}$$

where K_i are the eddy mass diffusivity coefficients in the i-th coordinate.

The K_i are related with the eddy viscosity ν_t by the following expression:

$$K_i = \nu_t / Sc_{t,i}, \tag{2.3}$$

where

$$\nu_t = c_\mu k^2 / \varepsilon$$

and k and ε are the turbulent kinetic energy and its dissipation rate, c_μ is an empirical constant in $k - \varepsilon$ turbulence closure scheme. In the equation (2.3), $Sc_{t,i}$ is the turbulent Schmidt number. The subscrip i implies that this number may be varied according to the directions.

In general, the turbulent Schmidt number is set equal to 0.9 in all directions in most of study (see [22]-[25]), i.e.:

$$Sc_{t,x} = Sc_{t,y} = Sc_{t,2} = 0.9. \tag{2.4}$$

3. Numerical solution method

The numerical solution uses centered difference schemes for the diffusion and source terms and a hybrid differencing scheme for the convection terms. In the solution of flow field, the SIMPLE algorithm was used (see [27], [28]).

As it is known, in the solution of the concentration equations with a point source of pollutant, the gradients of concentration is very high, especially in the region near the source, so a greater discretization error would be expected. However, at the same time, the solution of this concentration equation is much "cheaper" (required less CPU time) than the one of the flow field equations. Therefore, a higher-order but more "expensive" differencing scheme for the convection terms in the solution of concentration equation can be employed. This scheme combines the central differencing scheme (CDS) and upwind differencing scheme (UDS) in the following way [27]:

$$F = F^{UDS} + (F^{CDS} - F^{UDS})^{old},$$

where F^{UDS} and F^{CDS} stand for the approximations by the UDS and CDS, respectively. The terms in the brackets are evaluated by using values from the previous iteration. This scheme has not got the false diffusion like the CDS, in the same time it is stable like the UDS.

4. Verification of numerical models

4.1. Simulation results of the flow field

To verify the numerical model, the numerical simulations have been performed and compared with available measurement data from a physical model on airflow around a three-dimensional hill of conic shape [29].

The comparisons between the measured and calculated flow-field have been described in [30]. The findings can be summarized as follows (see [30] for details):

- The simulated mean flow velocities agree well with the measurements. Moreover, the results of the mean velocities are insensitive to the turbulence models used.

- In predicting the mean velocities and the turbulence in the outer region (region above surface region), all three models work well.

- In predicting the turbulence near the surface, there are discrepancies either among the calculation results or between them and the measurements. The simulated results for the turbulence depend strongly on the turbulence model used. Generally, the with Duynkerke's modifications yields the best agreement with measurements.

These calculated flow-fields will be used to calculate the respective concentration fields.

4.2. Description of the dispersion experiments

The experimental model of VKI was described in [23]. In addition to the measurements of the flow field (velocity vector), the pollutant concentration measurement was also made in the VKI experiments. The stack in this experimental model was located at a distance of $3.7H$ upstream from the center of the hill (H is the height of the hill) i.e. $x_s = -3.7H$ and $y_s = 0$. Two measurements of the concentration field were performed for the stack height $h_s = H/2$ and H. These measured and calculated concentrations were normalized as the following manner:

$$\chi = CU_eH^2Q^{-1}, \tag{4.1}$$

where χ = Normalized concentration; C = Concentration; U_e = Free stream velocity (velocity of flow before its entrance into the towing tank); H = Hill height and Q = Rate of source (g/s).

The measurements of the concentrations above the crest of the hill ($x = 0, y = 0$) were made in these experiments.

4.3. Calibration and verification of model from the experiments

Because the simulated flow and turbulence fields of Duynkerke's model agree with measurement better than two remainders, so this model was used to perform numerical simulations presented in this study. Many numerical simulations were performed with different eddy mass diffusivity coefficient. Results of this numerical simulation indicated, that the variation of eddy mass diffusivity coefficients has a strong influence on the concentration field. It may be expected that reasonable non-isotropic (especially between horizontal and vertical directions) eddy mass diffusivity will make the calculated results better. In fact, the turbulent diffusion process is more or less non-isotropic in the atmospheric boundary layer because of the big differences of its characteristics in horizontal and vertical dimensions due to ground

surface and action of Archimedian force. Therefore, the Schmidt numbers were used for calibration.

Based on the important assumption of the $k - \varepsilon$ model, which suggests, that the eddy diffusivity coefficients are proportional to ν_t, it can be expected that the Schmidt numbers in different directions may be different. It is naturally proposed that the non-isotropy be occurred only between horizontal and vertical directions because there is not any evident reason for the difference between two horizontal directions. Therefore two parameters changed in our matching are $Sc_{t,y}$ and $Sc_{t,z}$. The parameter $Sc_{t,x}$ was always set equal $Sc_{t,y}$.

The experimental data in the case $h_s = H$ were used for the calibration. The matching procedure is carried out in two steps:

- In first step, $Sc_{t,y}$ and $Sc_{t,z}$ were varied in the range from 0.5 to 1.5 with step 0.1. The closest agreement with the experiment data in this step was found in the case of $Sc_{t,y} = 0.6$ and $Sc_{t,z} = 0.8$.

- In second step, $Sc_{t,y}$ was varied around 0.6 (from 0.51 to 0.69 with step 0.01) and $Sc_{t,z}$ was varied around 0.8 (from 0.71 to 0.89 with step 0.01). Finally, the closest agreement with the experiment data was found in the case of $Sc_{t,y} = 0.61$ and $Sc_{t,z} = 0.83$ (see Fig. 1).

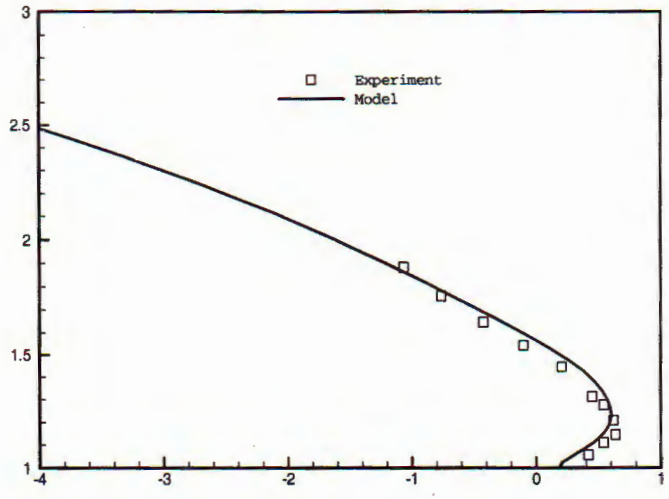

Fig. 1. Vertical concentration profiles above the crest of hill in the case of nonisotropic eddy mass diffusivity: $Sc_{t,x} = Sc_{t,y} = 0.61$; $Sc_{t,z} = 0.83$ and $h_s = H$, z/H vs normalized concentration (log)

A verification of obtained Schmidt numbers was performed for the case of $h_s = H/2$. Fixed the Schmidt number $Sc_{t,x} = Sc_{t,y} = 0.61$; $Sc_{t,z} = 0.83$, we have calculated the concentration and obtained satisfied result as shown in Fig. 2.

Investigation of the role of nonisotropic turbulent diffusivity for mass equations has been performed by some authors. For example, in a study of flow and dispersion around the cube, Zhang et al [26] selected $Sc_{t,x} = 0.77$, $Sc_{t,y} = 0.55$ and $Sc_{t,z} = 0.77$ after a matching with the experimental results of flow and dispersion around a cube.

In this study, we also performed matching with the experiment to explore a scheme of suitable turbulent Schmidt numbers. From our matching result ($Sc_{t,x} = 0.61$, $Sc_{t,y} = 0.61$ and $Sc_{t,z} = 0.83$) and the matching result of Zhang et al, it can be concluded that the turbulent Schmidt numbers seem to be less than the value of 0.9, which was used in most studies. It can be also concluded that the turbulent Schmidt numbers for horizontal directions may be less than this one for vertical direction.

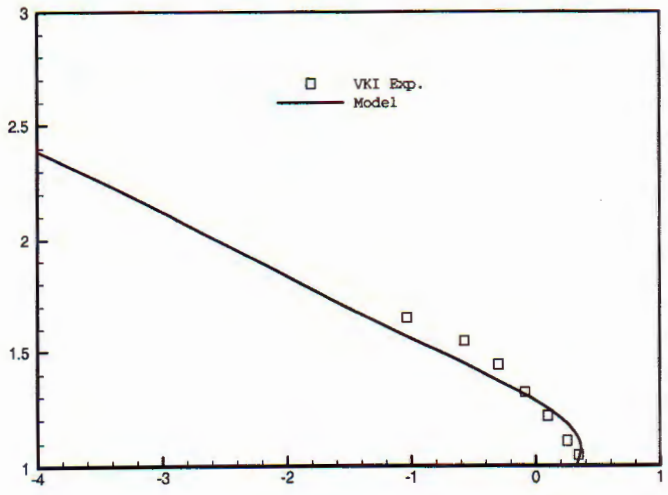

Fig. 2. Vertical concentration profiles above the crest of hill in the case of nonisotropic eddy mass diffusivity: $Sc_{t,x} = Sc_{t,y} = 0.61$; $Sc_{t,z} = 0.83$ with $h_s = H/2.z/H$ vs normalized concentration (log)

5. Effects of recirculation zone behind a building on pollutant transport and diffussion

5.1. Flow field simulation

Numerical experiments are performed for flow around a cubical building. The building height and widths are 60 m. The approach flow is perpendicular to one of building's sides. The following logarithmic wind law has been used for the approach flows:

$$\frac{u_0(z)}{u_{*0}} = \frac{1}{\kappa}\ln\Big(\frac{z-d}{z_0}\Big), \tag{5.1}$$

where: u_{*_0} is the friction velocity; κ is the von-Karman constant (~ 0.41); z_0 is the aerodynamic roughness length and is the zero-plane displacement.

The values of $u_{*_0} = 0.15\,\mathrm{m/s}$ and $z_0 = 0.001\,\mathrm{m}$ are used in the flow field simulation using the $k - \varepsilon$ model with the Duynkerke's modification. The velocity vectors in the vertical plane through the center of the building are shown in Fig. 3. In according to the calculation, the length of the recirculation zone behind building $L_R = 2.335H$. Here the length of the recirculation zone refers to the distance from the lee face of building to the farthest point at which the velocity was reversed. More details about the flow field simulation were presented in [31].

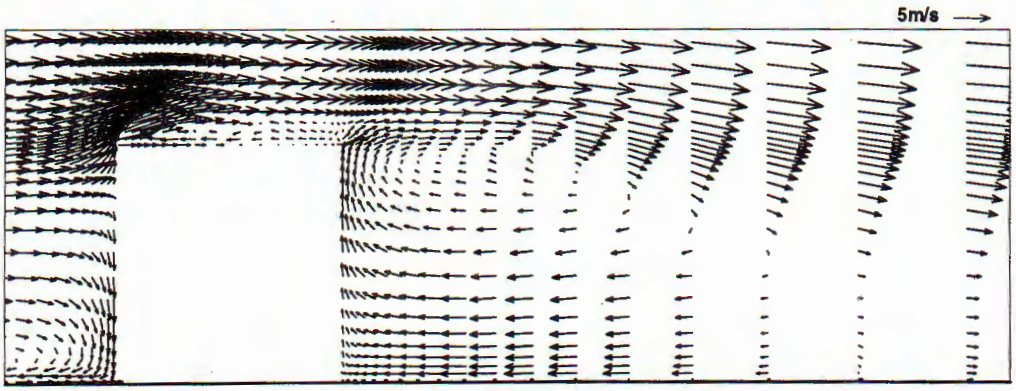

Fig. 3. Velocity vector field in the vertical plane through the center of building

5.2. Concentration field simulation

The simulated flow field, which is described previously, is used to simulate concentration fields. The stack was set in the vertical plane through the center of building. The rate of source is equal to 0.1 kg/s. However, in reality, the normalized concentration (4.1) is not dependent on the rate of source. The pollutants released are assumed passive. The numerical simulations were performed for stack located in different places near and behind the building. The concentration field simulation used a grid finer than the grid of flow field simulation. The flow field is interpolated from the flow field grid to concentration field grid. For each concentration simulation, the cells of the concentration field simulations has the side of $\frac{1}{30}H$ in a cubic region spread out from the point source at distances equal H in all directions. Out of this region, the sides of cells gradually increase in each direction. The ratio between two sides of two contiguous cells is equal to 1.1. The result of concentration fields and some concerned discussions will be presented in the following sections.

5.3. Effect on the recirculating of pollutants

It was expected that the pollutants, which are released inside a recirculation

zone, would be partly trapped in this zone. In this study, this effect was investigated numerically.

Firstly, to understand how the flow field affects on pollutant transport and dispersion more clearly, five following stacks are used in the numerical experiments:

- Stack case 1: $x_s = 0.5L_R$ and $z_s = 0.5H$
- Stack case 2: $x_s = 0.5L_R$ and $z_s = 0.85H$
- Stack case 3: $x_s = 0.5L_R$ and $z_s = 1.2H$
- Stack case 4: $x_s = 0.85L_R$ and $z_s = 0.5H$
- Stack case 5: $x_s = 1.2L_R$ and $z_s = 0.5H$

where x_s is the distance from stack to building and z_s is the height of stack (For all cases presented in this study $y_s = 0$).

For the stack case 1 (SC1), the concentration contours in the central vertical plane are shown in Fig. 4. To show the effect of recirculation zone more clearly, another numerical simulations are also performed with the same approach flow and the same emission source but without the building (i.e. in the flat terrain). The concentration contours in the case of flat terrain are show in Fig. 5.

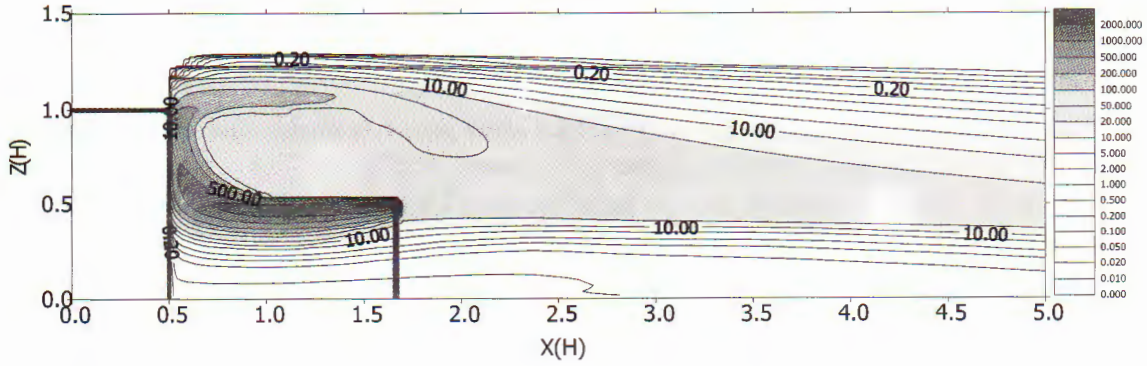

Fig. 4. Concentration contours in the vertical plane through the center of the building for the case of $x_s = 0.5L_R \approx 1.17H$ and $z_s = 0.8H$ (SC1)

Fig. 4 and 5 show that the recirculation zone strongly influences on the distribution of pollutants. With the existence of the building, the concentration distribution is controlled mainly by the vortex, which makes a quite large portion of pollutants trapped in the recirculation zone. The concentrations in the neighborhood of the stack are much higher than the similar value in the case of flat terrain.

To evaluate above-mentioned effect more quantitatively, in this study, results are compared using the total amount of pollutants contained in a recirculation box. Here, the recirculation box is defined as the box, which is located just behind the building, has the same width and thickness as the building and the same length as the recirculation zone L_R. This box is used to represent the real recirculation zone because the boundaries of recirculation zone are very difficult to determine exactly. The received results indicated that, in the case of $x_s = 0.5L_R$ and $z_s = 0.8H$, the

total amount of pollutant in the recirculation box is equal to 10.35 kg, whereas this one is only equal to 1.42 kg if the building does not exist. The quantitative comparison indicates that the recirculation zone strongly keeps the pollutants, therefore this action may make the concentration in the recirculation zone to be much higher than simular value in the case of flat terrain.

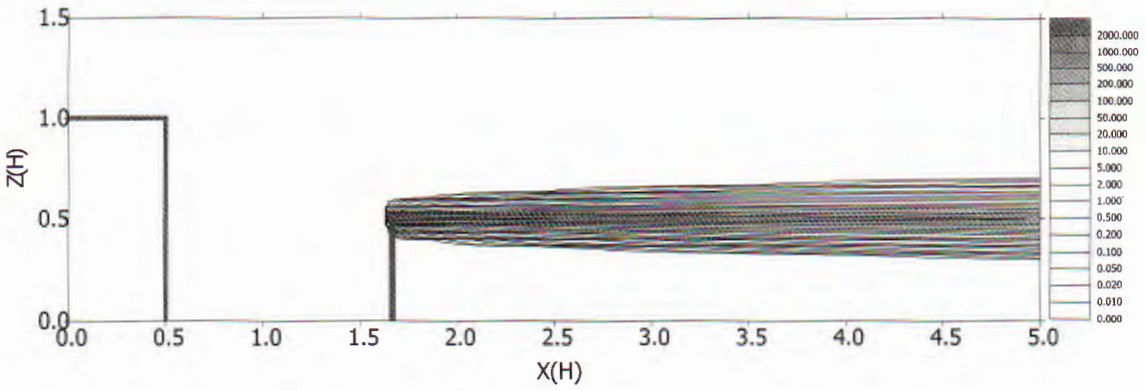

Fig. 5. Concentration contours in the vertical plane through the center of the building in the case of flat terrain

For the stack case 2 (SC2: $x_s = 0.5L_R$ and $z_s = 0.85H$), the concentration contours in the central vertical plane are shown in Fig.6. The total amount of pollutant in the recirculation box is equal to 19.27 kg, i.e. much greater than the similar value of SC1.

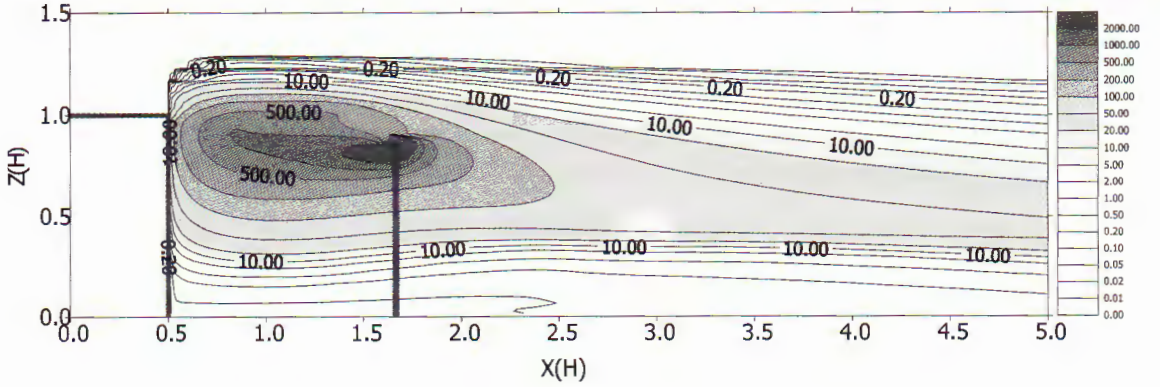

Fig. 6. Concentration contours in the vertical plane through the center of the building for the case of $x_s = 0.5L_R \approx 1.17H$ and $z_s = 0.85H$ (SC2)

The difference of the main path way of pollutant between SC1 and SC2, as shown in Fig. 4 and 6, can explain their difference of the total amount of pollutant

in recirculation box: In SC1, the emission point is located in a region with strong reversed velocities. The released pollutants, which are driven by the flow field, firstly were transported backward and then, after the plume of pollutant faced the building, strongly transported upward. This upward strong transport of pollutants can make a portion of pollutants escape from the recirculation zone. Whereas the emission point of the stack in SC2 is located near the center of main vortex, so the pollutants escape from the recirculation zone more difficult.

For the stack case 3 (SC3: $x_s = 0.5L_R$ and $z_s = 1.2H$), the concentration contours in the central vertical plane are shown in Fig. 7. As shown in Fig. 7, the emission point in SC3 is located outside the recirculation zone, so the plume of pollutants is mainly advected far away. Only a small portion of pollutants is recirculated and the total amount of pollutants (equal 0.75 kg) is much smaller than the similar value for the stack case 1 and 2.

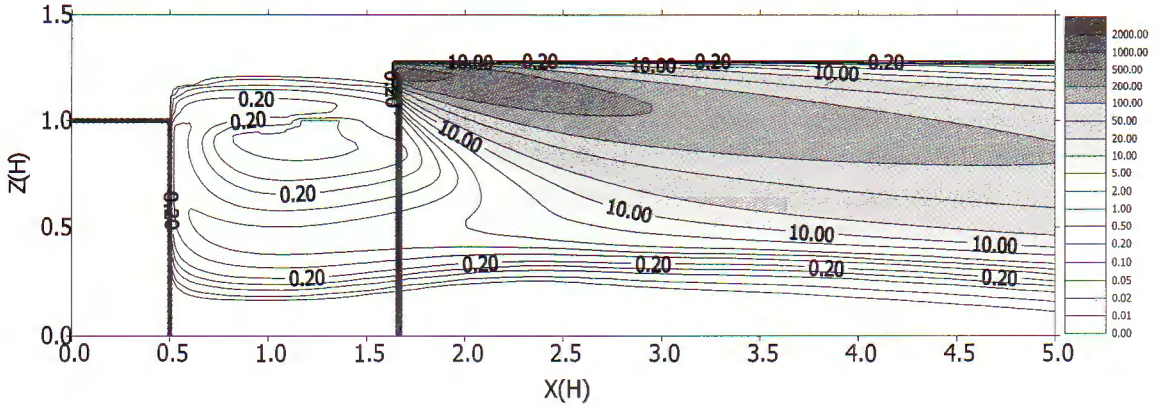

Fig. 7. Concentration contours in the vertical plane through the center of the building for the case of $x_s = 0.5L_R \approx 1.17H$ and $z_s = 1.2H$ (SC3)

For the stack case 4 (SC4: $x_s = 0.85L_R$ and $z_s = 0.5H$), the concentration contours in the central vertical plane are shown in Fig. 8. The stack in SC4 has the same height as this one in SC1, but is located at a father distance from the building. For this case, the total amount of pollutant in the recirculation box is equal to 13.3 kg, i.e. greater than the similar value in SC1. The slight difference of the main pathway of pollutant between SC1 and SC4, as shown in Fig. 4 and 8, can explain their difference of the total amount of pollutant in recirculation boxes. In both SC1 and SC4, the emission points are located in a region with strong reversed velocities. The released pollutants, after the plume of pollutant faced the building, are strongly transported upward. The pollutant pathway to the top of recirculation zone in SC4 is longer than the one in SC1, therefore, the portion of pollutant escapes from the recirculation zone in SC4 is smaller than the one in the SC1.

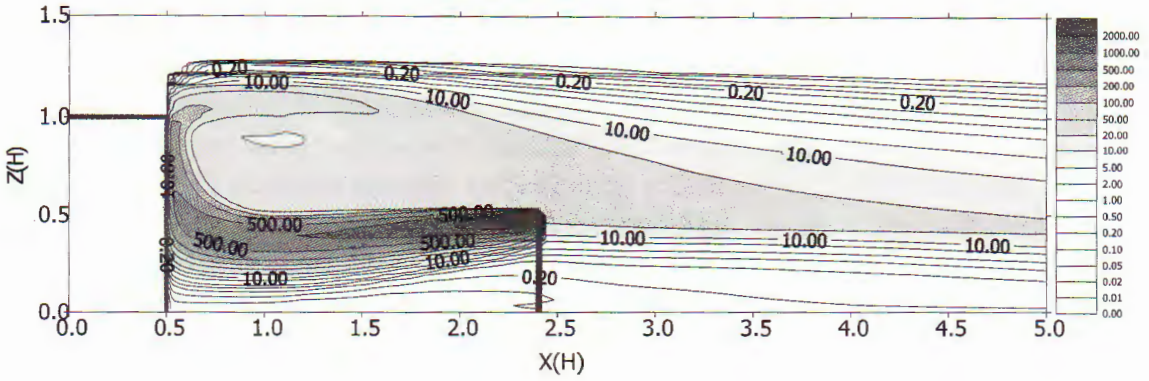

Fig. 8. Concentration contours in the vertical plane through the center of the building for the case of $x_s = 0.85L_R \approx 1.98H$ and $z_s = 0.5H$ (SC4)

For the stack case 5 (SC5: $x_s = 1.2L_R$ and $z_s = 0.8H$), the stack is located outside the recitculation zone. The concentration contours in the central vertical plane are shown in Fig.9. It can be seen in Fig. 9 that the pollutants are not transported into the recirculation zone. However, from the comparison between Fig. 9 and Fig. 5 (for the case of flat terrain), the existence of building make the transport of pollutant more downward. Because of this, the ground-level concentration may be higher than this one in the case of flat terrain.

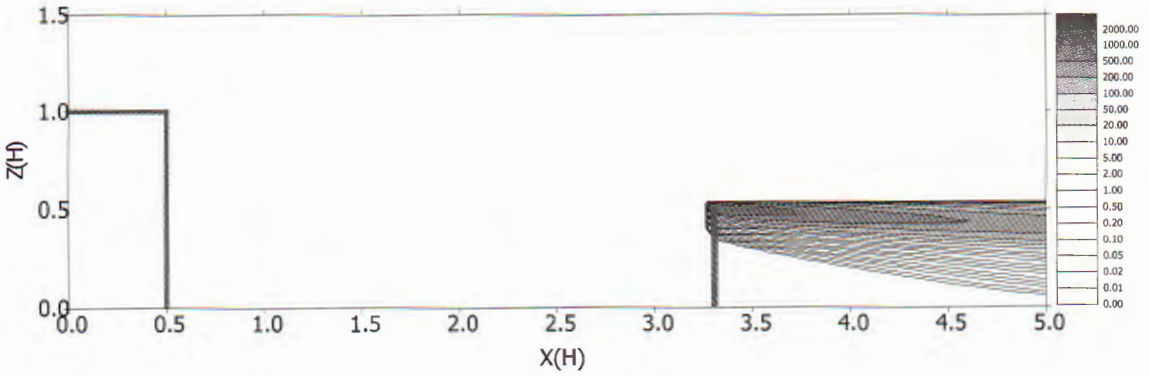

Fig. 9. Concentration contours in the vertical plane through the center of the building for the case of $x_s = 1.2L_R \approx 2.8H$ and $z_s = 0.5H$ (SC5)

In addition to SC1, SC2 and SC3, series of numerical experiments was performed for some stacks with the same location ($x_s = 0.5L_R \approx 1.17H$). The heights of these stacks vary in the range from $0.1H$ to $2H$. The dependence of the total amount of pollutants in recirculation box is shown in Fig. 10. In this figure, the total amounts of pollutants associated with flat terrain are also presented in order to have quantitative evaluations.

It can be seen in Fig. 10, the total amount of pollutants in the recirculation box increases as the stack height increases from $0.1H$ to $0.8H$, and rapidly decreases as the stack height continually increases and nearly equals zero as the stack height greater than $1.3H$. From the vector field presented in Fig. 3, it can be realized that the recirculating of pollutants will become strong as the emission point near the center of the main vortex.

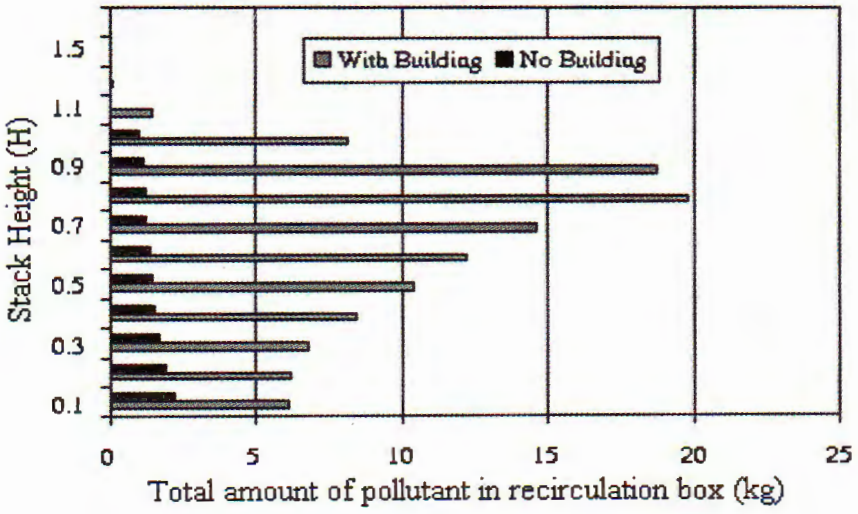

Fig. 10. Total amount of pollutant as a function of the stack height for the cases $x_s = 0.5L_R$

Another series of numerical experiments were also performed for some other stacks, which have the same height as SC1, SC3 and SC4 ($Z_s = 0.5H$), but are located at different distances from the building. The distance from stack to building x_s varies in the range from $0.1H$ to $3H$ ($\sim 1.3L_R$). The total amounts of pollutants in the recirculation box, together with the similar ones in the case of flat terrain, are presented in Fig. 11.

As shown in Fig. 11, the total amount of pollutants slightly increases as x_s increases from 0 to about $0.8L_R$ ($\sim 1.86H$), rapidly decreases as x_s continually increases and nearly equal zero when the stack are located outside the recirculation zone ($x_s \geq L_R = 2.33H$). From the vector field presented in Fig. 3, it can be realized that the recirculating of pollutants will become strong when the flow near the emission point becomes downward.

6. Conclusions

The first purpose of this study was to develop and verify a three- dimensional numerical model of the atmospheric transport and diffusion of pollutants over a complex terrain. The code, incorporating a more accurate turbulence closure model

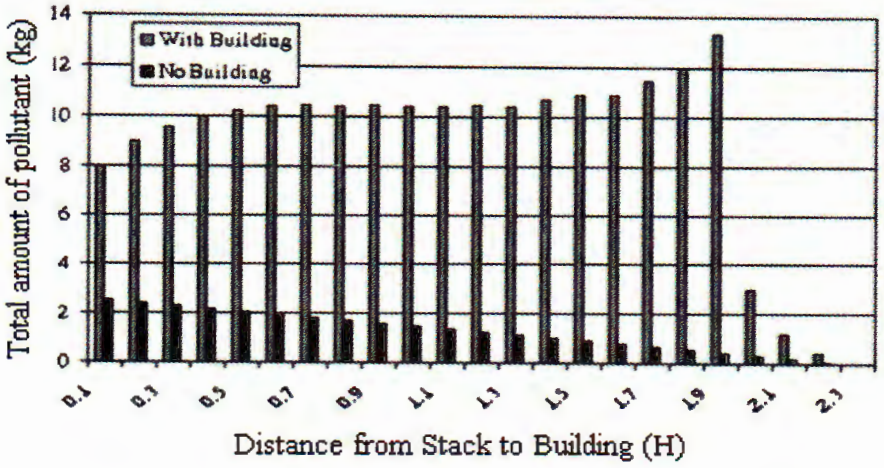

Fig. 11. Total amount of pollutant as a function x_s for the case $z_s = 0.5H$

than normally used in atmosphere pollution model, was developed for simulations of pollutant transport near an obstacle. The results of numerical simulation are compared with available measurements conducted by von-Karman Institute of Fluid Dynamics (Belgium). Based on the results and evaluations of the simulations, the following conclusions can be drawn:

- The model appeared to be suitable for solving a complicated problem of pollutant transport over a complex terrain. The calculation CPU time is also suitable for real capability of PC.

- The simulated concentration field is highly sensitive to the specification of eddy mass diffusivity. A nonisotropic dispersion model based on $k - \varepsilon$ turbulence closure scheme with $Sc_{t,x} = Sc_{t,y} = 0.61$ and $Sc_{t,z} = 0.83$ gave the calculation results agreed well with the VKI experiment.

The second purpose of this study concerns the influences of the recirculation zone behind an obstacle - a cubical building on the transport and diffusion of pollutants when a stack is set in these zones. The study focuses on the effects of location of the source, in the relation with the flow field, on the recirculating of pollutants. The recirculation of pollutant was investigated using the total amount of pollutants in the recirculation box, which are used like a representative of the recirculation zone. The numerical investigations indicated that:

- The pollutants, which are released from a source near and behind a building, may be partly trapped in the recirculation zone. This effect makes the total amount of pollutants in the recirculation box becomes very high. Depending on stack location and height, this amount is greater than the similar one in the cases of flat terrain from 3 to 30 times.

- The effect of building on the recirculation of pollutants will be unnoticeable when the stack height is greater than the building height about 1.2 times or when the distance from the stack to the building greater than the length of recirculation zone.

- The effect of building on the recirculation of pollutants will become very strong when the emission point is located near the center of main vortex or when the flow near the emission point is downward strongly.

The model can be developed, adapted and used for different research and applied purposes.

The study is implemented partly with the financial support from the Vietnam National Council of Natural Sciences.

REFERENCES

1. Genikhovich E. L. and Schiermeier F. A. Comparison of United States and Russian Complex Terrain Diffusion Models Developed for Regulatory Applications. Atmos. Environ., Vol. 29, No. 17, 1995, pp. 2375-2385.
2. Turner D. B., Bender L. W., Pierce T. E. and Petersen W. B. Air Quality Simulation Models from EPA. Environ. Software, Vol. 4, No. 2, 1989, pp. 52-61.
3. Perry S. G. CTDMPLUS: A Dispersion Model for Source near Complex Topography. Part I: Technical Formulations. J. Appl. Meteoro., Vol. 31, pp 633-644, 1992.
4. Ros D. G., Fox D. G. Evaluation of an Air Pollution Analysis System for Complex Terrain, J. App. Meteor., Vol. 30, pp. 909-922, 1991.
5. Sherman C. A., A Mass-Consistent Model for Wind Fields over Complex Terrain. J. App. Meteor. Vol. 17: 312-319, 1978.
6. Garrat J. R. The atmospheric boundary layer. Cambridge University Press, New York, 1992.
7. Mellor G. L. and Yamada T. A Hierarchy of Turbulence Closure Models for Planetary Boundary Layers. J. Atmos. Sci., Vol.31, pp. 1791-1806, 1974.
8. Lyons T. J. and Scott W. D. Principles of Air Pollution Meteorology. Belhaven Press, London, 1990.
9. Physick W. L. et al. LADM: A Lagrangian Atmospheric Dispersion Model. CSIRO Division of Atmospheric Research Technical Paper No.24, CSIRO Australia, 1994.
10. Duong Ngoc Hai, Nguyen The Duc. Assessment of the air quality impacts arising from operation of the Quang Ninh Thermal Power Plant. Proc. of the VI-th National Conference on Mechanics, Hanoi, 1997.
11. Duong Ngoc Hai, Nguyen Van Diep, Nguyen The Duc, Le Trinh. Wind Field over Complex Terrain and Air Quality Modeling. J. Mechanics, NCNST of Vietnam, T.XIX, 1997, No 4, pp. 29-38.

12. Bellasio R. and Tamponi M. MDGP: A new Eulerian 3D unsteady state model for heavy gas dispersion. Atmos. Environ., Vol. 28, No. 9, pp. 1633-1643, 1994.
13. Jacbson M. Z., Lu R., Turco R. P. and Toon O. B. Development and Application of a new Air Pollution Modelling System - Part I: Gas-Phase Simulation. Atmos. Environ., Vol. 30, No. 12, pp. 1939-1963, 1996.
14. Yao C., Arya S. P., Davis J. and Main C. E. A numerical model of the transport and diffusion of peronospora tabacina spores in the evolving atmospheric boundary layer. Atmos. Environ., Vol. 31, No. 11, pp. 1709-1714, 1997.
15. Mellor G. L. and Herring H. J. A Survey of the Mean Turbulent Field Closure Models. AIAA Journal, Vol. 11, No. 5, pp. 591-599, 1973.
16. Lumley J. L. Second Order Modeling of Turbulent Flows. In Prediction Methods for Turbulent Flows, Ed. by Kollmann W., Hemisphere Publishing Corporation, Washington, 1980.
17. Rodi W. Turbulence Models for Enviromental Problems. In: Prediction Methods for Turbulent Flows, Ed. by Kollmann W., Hemisphere Publishing Corporation, Washington, 1980.
18. Detering, H. W., and D. Etling. Application of the Turbulence Model to the Atmospheric Boundary Layer. Bound. Layer Meteor., Vol. 33, 1985, pp. 113-133.
19. Duynkerke P. G. Application of the Turbulence Closure Model to the Neutral and Stable Atmospheric Boundary Layer. J. Atmos. Sci., Vol. 45, 1988, pp. 865-880.
20. Duong Ngoc Hai, Nguyen The Duc. A Three Dimensional Non-Hydrostatic Model for Turbulent Air Flow. J. Mechanics, Vol.22, No. 3, 2000.
21. Duong Ngoc Hai and Nguyen The Duc. An Evaluation About Two Modifications of the Standard Model for Numerical Simulation of Turbulent Air Flow. Proceeding of 2-nd International Symposium on Modeling Simulation. Hanoi, Dec., 2000.
22. Aspley D. D. and Castro I. P. Numerical Modelling of Flow and Dispersion around Cinder Cone Butte. J. Atmos. Environ., 31(7), pp. 1059-1071, 1996.
23. Sini J. F., Anquetin S. and Mestayer P. G. Pollutant Dispersion and Thermal Effects in Urban Street Canyons, J. Atmos. Environ., 30(15), pp. 2659-2677, 1996.
24. Kim J. J. and Baik J. J. A Numerical Study of Thermal Effects on Flow and Pollutant Dispersion in Urban Street Canyons. J. Appl. Meteo., 38(9), pp. 1249-1261, 1998.
25. Baik J. J. and Kim J. J. A Numerical Study of Flow and Pollutant Dispersion Characteristics in Urban Street Canyons, J. Appl. Meteo., 38(11), pp. 1576-1589, 1999.

26. Zhang Y. Q. and S. P. Arya, A Comparision of Numerical and Physical Modelling of Stable Atmospheric Flow and Dispersion around a Cubical Building, J. Atmos. Environ., 30(8), 1996, pp. 1327-1345.
27. Ferziger J. H. and M. Peri D. Computational Methods for Fluid Dynamics. Springer Press, 1996.
28. Patankar S. V. Numerical Heat Transfer and Fluid Flow. McGraw-Hill, New York, 1980.
29. Costa M. J., Riethmuller M. L. and Borrego C. Wind-Tunel Simulation of Gas Dispersion over Complex Terrain: Comparison of Two Length-Scale Studies. Atmos. Environ., Vol. 28, No. 11, 1994, pp. 1933-1938.
30. Duong Ngoc Hai, Nguyen The Duc. Three Dimensional Non-Hydrostatic Model of Turbulent Atmospheric Boundary Layer. In: Proc. of the 8-th Intern. Symposium on Flow Modelling and Turbulent Measurement, Tokyo - FMTM 2001, World Scientific Pub. Co., 2002.
31. Duong Ngoc Hai, Nguyen The Duc. Numerical study of the recirculation zone behind a building in the neutral and stable atmospheric boundary layer. J.Mechanics, Vol. 24, No.2 , pp. 1-20, 2002.

Received June 10, 2002

MÔ PHỎNG SỐ SỰ VẬN CHUYỂN VÀ PHÁT TÁN CHẤT GÂY Ô NHIỄM GẦN VẬT CẢN TRÊN CƠ SỞ SƠ ĐỒ ĐÓNG KÍN RỐI $k - \varepsilon$

Để mô phỏng trường gió và sự vận chuyển, phát tán chất gây ô nhiễm gần vật cản đã xây dựng chương trình tính toán trên cơ sở mô hình $k - \varepsilon$. Bên cạnh mô hình chuẩn, đã xem xét 2 biến thể do Detering & Etling và Duynkerke đề xuất. Kết quả tính toán được kiểm chứng bằng cách so sánh với số liệu đo đạc của Viện Thủy động lực học von Karman (Bỉ). Như một tham số hiệu chỉnh mô hình, để làm phù hợp với các kết quả đo đạc, đã áp dụng tính toán với các số Schmidt rối khác nhau. Chương trình tính toán được sử dụng nghiên cứu sự ảnh hưởng của vùng quẩn sau vật cản hình hộp lên sự vận chuyển và phát tán chất gây ô nhiễm. Đã nghiên cứu ảnh hưởng của vị trí và độ cao của ống khói lên quá trình xem xét.

Institute of Mechanics, NCNST
264, Doican Str., Hanoi, Vietnam
Email: dnhai@im01.ac.vn